Supplementary Information: "PNIPAm microgels under alcoholic intoxication: When a LCST polymer shows swelling with increasing temperature"

Sebastian Backes,[†,‡] Patrick Krause,[†] Weronika Tabaka,[†] Marcus U. Witt,[†,‡]

Debashish Mukherji,[¶] Kurt Kremer,[¶] and Regine von Klitzing[*,†,‡]

Stranski-Laboratorium für Physikalische und Theoretische Chemie, Technische Universität Berlin, Straße des 17. Juni 124, 10623 Berlin, Germany, Institut für Physik, Technische Universität Darmstadt, Alarich-Weiss-Strasse 10, 64287 Darmstadt, Germany, and Max-Planck-Institut für Polymerforschung, Ackermannweg 10, 55128 Mainz, Germany

E-mail: klitzing@fkp.tu-darmstadt.de

This supporting information contains details about the material synthesis, dynamic light scattering (DLS), dynamic force measurements, and the all-atom molecular dynamics simulations. Additonally, we also provide a few figures to support the claims presented in the main manuscript text.

Materials

For the synthesis of PNIPAm microgels, we have used N,N'-methylenbisacrylamide (BIS) as cross-linker. N-isopropylacrylamide (NIPAM), acrylic acid (AAC), N,N'-methylenbisacrylamide (BIS),

---

[*]To whom correspondence should be addressed

[†]Stranski-Laboratorium für Physikalische und Theoretische Chemie, Technische Universität Berlin, Straße des 17. Juni 124, 10623 Berlin, Germany

[‡]Institut für Physik, Technische Universität Darmstadt, Alarich-Weiss-Strasse 10, 64287 Darmstadt, Germany

[¶]Max-Planck-Institut für Polymerforschung, Ackermannweg 10, 55128 Mainz, Germany

and potassium persulfate (KPS) that were purchased from Sigma-Aldrich. The ethanol (absolute), methanol, and 2-propanol were purchased from Chem-solute. For the water purification a three stage millipore system (Milli-Q Plus 185) was used.

Synthesis

For the synthesis a surfactant free precipitation polymerization was used. The protocol for synthesis is taken from the published work.[1] Both gels, PNIPAM and PNIPAM-co-AAc, were synthesized with the negative initiator KPS. The PNIPAM monomers, AAc comonomers and cross-linker BIS were dissolved in Milli-Q water and the solution was degassed for 60 min with nitrogen under constant stirring. The solution was transferred into a reactor and heated to 70°C. The initiator KPS was dissolved in 2 Milli-Q water and 1 ml ($\widehat{=}$5.5 mmol/l) was transferred into the reactor to start the polymerization. The reaction volume was cooled after 90 min of reaction time in a separate beaker in an ice bath. At room temperature, the microgel was purified by dialysis against Milli-Q water for 10 days. The microgels were freeze-dried at -85°C. Both gels contain 4.8% cross-linker, and PNIPAM-co-AAc additionally contains 5% AAc.

DLS measurements

The hydrodynamic radius R_h of microgels in bulk solution was measured by dynamic light scattering (DLS). Measurements were performed on an LS spectrometer (LS Instruments, Fribourg, Switzerland) with a HeNe laser at λ=632.8 nm with 21 mW. For the correlation function the LS spectrometer was used. The scattering intensity was measured for 30 s at angles between 30° and 120° in steps of 5°. In temperature dependent measurements all samples were heated from 14°C to 60°C and then cooled again in steps of 2°C. The data were fitted using a self-written script with the cumulant fit procedure. Figure S1 shows the change in R_h with changing T for different volume fraction of ethanol volume fraction ϕ_e. The data is shown for both heating and cooling cycles. It can be seen that R_h with T does not show any hysteresis. Therefore, in the main manuscript text,
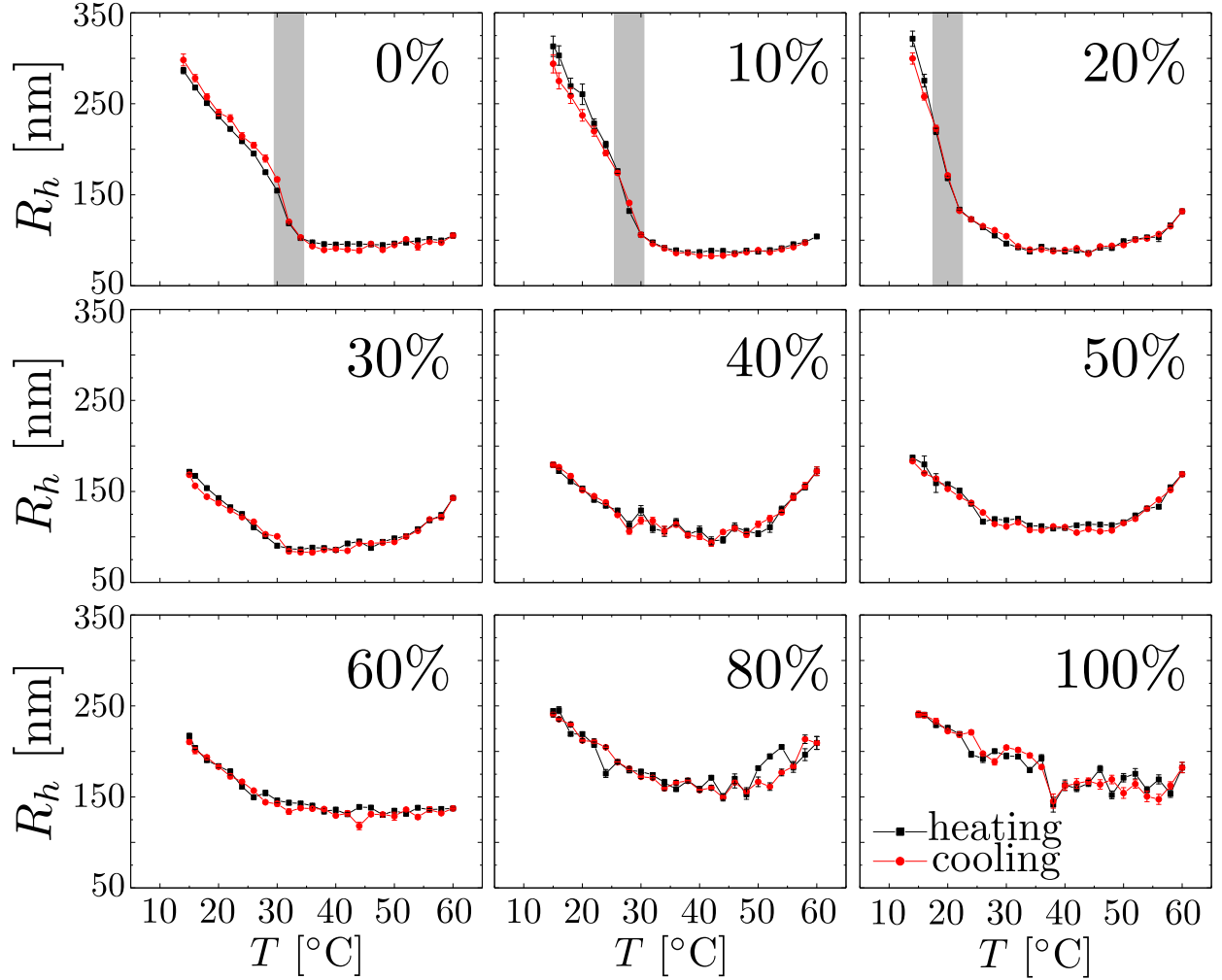
2

Figure S1: Hydrodynamic radius R_h of PNIPAM microgels against temperature T for different ethanol volume fractions ϕ_e. Both heating and cooling curves are shown. The grey bar indicates the VPTT for 0, 10, and 20% ethanol.

only the heating data are plotted.

In the main text, the data for $T = 20°C$ and $60°C$ are shown. To further illustrate the effect of ϕ_e on the plateau observed between $30°C$ and $50°C$, Figure S2 shows R_h against ϕ_e for $44°C$. It is evident from the plot that the preferential binding of ethanol with NIPAM monomers leads to an increase in plateau minima for $\phi_e > 20\%$.
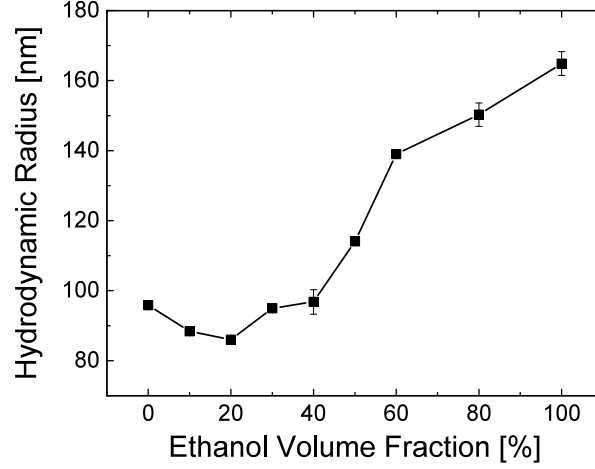
Figure S2: Hydrodynamic radius R_h of PNIPAM microgels measured by DLS as a function of ethanol volume fraction ϕ_e for $T = 44°$C.

Comparison of PNIPAM and Poly(NIPAM-co-AAC) microgels

For the measurement of stiffness on the surface, PNIPAM microgels with the comonomer acrylic acid (P(NIPAM-co-AAC)) are used because of their significantly larger size. Figure S3 shows a comparative plot of R_h as a function of ϕ_e and for $T = 20°$C.
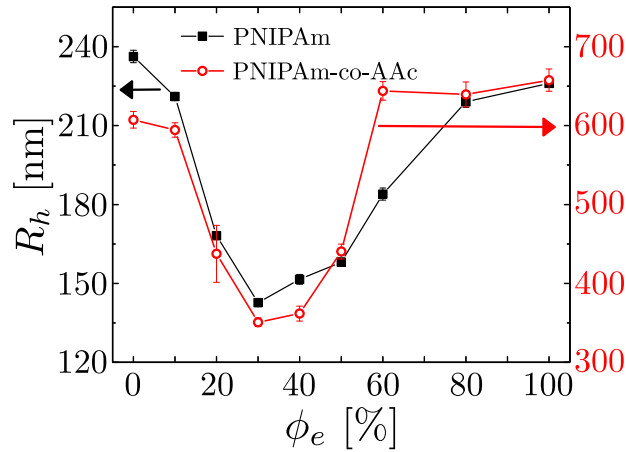

Figure S3: Hydrodynamic radii R_h of PNIPAM and P(NIPAM-co-AAC) microgels measured by DLS as a function of ethanol volume fraction ϕ_e for $T = 20°$C.

4

Solution preparation

Note that for the data shown here, samples have been produced by dissolving the microgels in the already prepared respective water-ethanol solutions. However, the results remain unaltered if the microgels are first dissolved in pure water or pure ethanol, and the cosolvent is added later, as shown in Figure S4. This suggests that there is no "memory effect" and the gels adapt their characteristic conformation in a given solvent mixing ratio irrespective of their previous state.
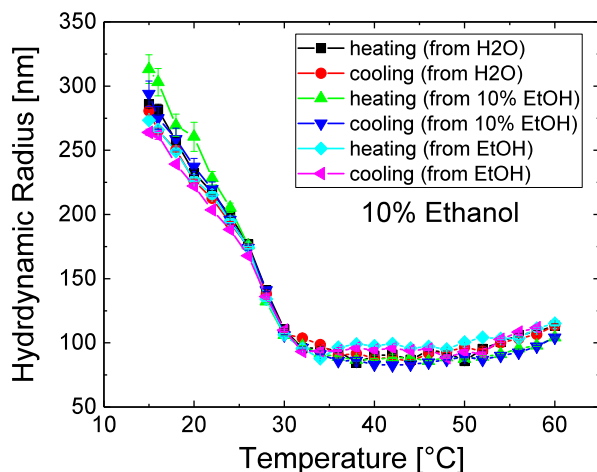

Figure S4: Hydrodynamic radii R_h as a function of temperature T for 10% volume fraction of ethanol. The samples were prepared by three different methods: first dissolving PNIPAM in water and adding ethanol later, first dissolving PNIPAM in ethanol and adding water later, and dissolving PNIPAM in the already prepared solution of water and ethanol.

Molecular dynamics simulations

In this work, the all-atom molecular dynamics simulation are performed using the GROMACS 4.6 package.[2] The force field parameter for PNIPAm is taken from Ref.[3] We have used the SPC/E water model[4] and OPLS force field for ethanol.[5]

The temperature is controlled using velocity rescaling[6] with a coupling constant 0.5 ps. The time step for the simulations is chosen as 1 fs. In a series of simulations, the temperature is varied from $-20°C$ to $65°C$. The simulations are performed with a constant pressure ensemble, where the pressure is controlled using a Berendsen barostat[7] with a coupling time of 0.5 ps and
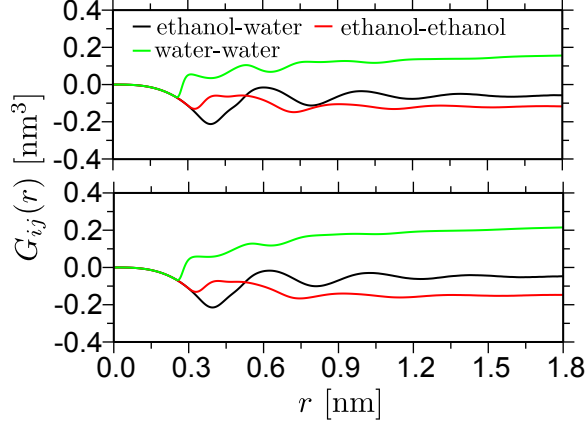
Figure S5: Kirkwood-Buff integral G_{ij} between ethanol-ethanol, ethanol-water, and water-water. Top panel is for the ambient conditions and the lower panel is for $T = 65°C$.

1 atm pressure. The electrostatics are treated using Particle Mesh Ewald.[8] The interaction cutoff is chosen as 1.0 nm. The chain length is chosen as $N_l = 32 \sim 12\ell_p$, with ℓ_p being the persistence length. The chain is solvated in a simulation box consisting of 3.0×10^4 solvent molecules for three different ethanol volume fractions ϕ_e. Each polymer configuration is simulated for 100 ns, where the data from the last 50 ns is used for the analysis. Note that the time scale of simulation is about one order of magnitude larger than the typical end-to-end distance R_e relaxation time $\tau \sim 3$ ns for $N_l = 32$, which is calculated using the auto-correlation function $\langle R_e(t) \cdot R_e(0) \rangle \sim e^{-t/\tau}$.

In the main text it is stated that the ethanol and water are well miscible at all temperatures. A quantity that gives a better estimate of the miscibility in a binary solution is the Kirkwood-Buff integral G_{ij}[9] that is written as,

$$G_{ij} = 4\pi \int_0^\infty \left[g_{ij}(r) - 1 \right] r^2 dr, \tag{1}$$

where $g_{ij}(r)$ is the pair distribution function between two components i and j, respectively. Figure S5 shows a comparative plot of G_{ij} between different solvent components and for two different temperatures. The information presented in Figure 5 can be translated into a preferential solvation parameter $\eta = G_{ee} + G_{ww} - 2G_{ew}$, which is equivalent to the effective $\chi \sim \eta/2$ parameter. From the data we find $\chi \sim 0.16$ for the ambient condition and $\chi \sim 0.23$ for $T = 65°C$. Note that for

phase separation $\chi \gg 1$, so the bulk solution remains stable for all temperatures.

References

(1) Pelton, R.; and Chibante, P. *Colloids Surf.* **1986**, *20*, 247.

(2) Pronk, S.; Pall, S.; Schulz, R.; Larsson, P.; Bjelkmar, P.; Apostolov, R.; Shirts, M.R.; Smith, J.C.; Kasson, P.M.; van der Spoel, D.; Hess, B.; Lindahl, E. GROMACS 4.5: a high-throughput and highly parallel open source molecular simulation toolkit. *Bioinformatics* **2013** *29*, 845.

(3) Walter, J.; Sehrt, J.; Vrabec, J.; Hasse, H. *J. Phys. Chem. B* **2012** *116*, 5251.

(4) Berendsen, H. J. C.; Grigera, J. R.; Straatsma, T. P. *J. Phys. Chem.* **1987 91**, 6269.

(5) Jorgensen, W. L.; Maxwell, D. S.; J. Tirado-Rives, J. *J. Am. Chem. Soc.* **1996** *118*, 11225.

(6) Bussi, G.; Donadio, D.; Parrinello, M. *J. Chem. Phys.* **2007** *126*, 014101.

(7) Berendsen, H. J. C.; Postma, J. P. M.; van Gunsteren, W. F.; DiNola, A.; Haak, J. R. *J. Chem. Phys.* **1984 81**, 3684(1984).

(8) Essmann, U.; Perera, L.; Berkowitz, M. L.; Darden, T.; Lee, H.; Pedersen, L. G. A. *J. Chem. Phys.* **1995** *103* 8577.

(9) Kirkwood, J. G.; Buff, F. P. *J. Chem. Phys.* **1951** *19*, 774.